PROCEEDINGS OF SCIENCE

Comparison Between ^{9}Li And ^{10}Be Nuclei from Viewpoint Of Nuclear Structure And Reaction

Takenori Furumoto*
Graduate School of Education, Yokohama National University, Yokohama 240-8501, Japan
E-mail: furumoto-takenori-py@ynu.ac.jp

Tadahiro Suhara

Matsue College of Technology, Matsue, Shimane 690-8518, Japan

Naoyuki Itagaki

Yukawa Institute of Theoretical Physics, Kyoto University, Kyoto 606-8502, Japan

Recently, we proposed the microscopic structure and reaction models. The model firstly constructs the nuclear structure by the stochastic multi-configuration mixing (SMCM) method based on the cluster model. Next, the cross section is obtained by the microscopic coupled-channel (MCC) calculation based on the folding model with the complex G-matrix interaction. In this work, we compare the ^{9}Li nucleus with the ^{10}Be nucleus from the viewpoint of the nuclear structure and reaction. The ^{9}Li (^{10}Be) nucleus is described as an $\alpha + t$ (α) $+ n + n$ four-body system based on the cluster model. The elastic and inelastic scattering cross sections for the ^{9}Li + ^{12}C and ^{10}Be + ^{12}C systems are obtained by the MCC calculation with the MPa interaction which is the latest version of the complex G-matrix interaction derived from the ESC nucleon-nucleon interaction model. The excitation energies of the low-lying states for the ^{9}Li and ^{10}Be nuclei well reproduce the data. The MCC model including the excitation effect of the projectile and target shows the visible channel coupling effect on the elastic cross section. The contribution of the ^{10}Be excitation effect is clearly larger than that of the ^{9}Li excitation effect.

The 26th International Nuclear Physics Conference
11-16 September, 2016
Adelaide, Australia

*Speaker.

PoS(INPC2016)224

1. Introduction

The α cluster structure in nucleus is known to have an important role to construct the heavy elements. The abundant heavy elements are produced through the triple α resonant state so-called Hoyle state. Nowadays, the exiting the various clusters (not only the α cluster but also the light and/or heavy clusters) is predicted in nucleus of the ground and excited states. Especially, the cluster structure in the light nuclei is noticeable and decoupling to the simple shell model structure.

The cluster features of the ^{10}Be and ^{9}Li nuclei have been frequently investigated from both nuclear structure and reaction viewpoints. In terms of the cluster model, the ^{10}Be (^{9}Li) nucleus is described as the $\alpha+\alpha(t)+n+n$ four-body systems, respectively [1, 2, 3, 4]. Recently, their similarity has been discussed from the viewpoint of the nuclear structure as in Refs. [4, 5, 6, 7]. However, their similarity is not investigated from the viewpoint of the nuclear reaction, although numerous observations are obtained through the nuclear reaction experiments.

In this paper, we investigate the similarity and/or dissimilarity of the ^{10}Be and ^{9}Li nuclei with the microscopic structure and reaction models. The model consists of the combination of the microscopic cluster model and the microscopic coupled channel (MCC) method. In the microscopic cluster model, the total wave function is composed of superposition of various cluster configurations. The transition densities are derived from the total wave function, and we use them for the elastic cross section calculations in the MCC framework. The channel coupling (CC) effects with the excited states are clearly shown for the ^{10}Be and ^{9}Li scatterings. Here we focus on the dissimilarity of the CC effect in the ^{10}Be and ^{9}Li nuclei.

2. Formalism

The detail calculation of the SMCM and MCC models is presented in Ref. [4]. Here, we briefly introduce the SMCM and MCC models.

First, we introduce basis states with various $\alpha+t+n+n$ ($\alpha+\alpha+n+n$) configurations, $\{\Psi_i^{J^\pi MK}\}$, to describe the ^{9}Li (^{10}Be) structure in the microscopic cluster model. The total wave function $\Phi^{J^\pi M}$ is therefore,

$$\Phi^{J^\pi M}=\sum_K\sum_i c_{i,K}\Psi_i^{J^\pi MK}. \tag{2.1}$$

The eigenstates of Hamiltonian are obtained by diagonalizing the Hamiltonian matrix, and the coefficients $\{c_{i,K}\}$ for the linear combination of Slater determinants are obtained.

The i-th basis state of $\{\Psi_i^{J^\pi MK}\}$ with the $\alpha+t+n+n$ ($\alpha+\alpha+n+n$) configuration has the following form. For the ^{9}Li nucleus,

$$\Psi_i^{J^\pi MK}=P^\pi P^{JMK}\mathscr{A}\left[\phi_\alpha(\boldsymbol{r}_1\boldsymbol{r}_2\boldsymbol{r}_3\boldsymbol{r}_4,\boldsymbol{R}_1)\phi_t(\boldsymbol{r}_5\boldsymbol{r}_6\boldsymbol{r}_7,\boldsymbol{R}_2)\ \phi_{n^{(1)}}(\boldsymbol{r}_8,\boldsymbol{R}_3)\phi_{n^{(2)}}(\boldsymbol{r}_9,\boldsymbol{R}_4)\right]_i, \tag{2.2}$$

for the ^{10}Be nucleus,

$$\Psi_i^{J^\pi MK}=P^\pi P^{JMK}\mathscr{A}\left[\phi_{\alpha^{(1)}}(\boldsymbol{r}_1\boldsymbol{r}_2\boldsymbol{r}_3\boldsymbol{r}_4,\boldsymbol{R}_1)\phi_{\alpha^{(2)}}(\boldsymbol{r}_5\boldsymbol{r}_6\boldsymbol{r}_7\boldsymbol{r}_8,\boldsymbol{R}_2)\ \phi_{n^{(1)}}(\boldsymbol{r}_9,\boldsymbol{R}_3)\phi_{n^{(2)}}(\boldsymbol{r}_{10},\boldsymbol{R}_4)\right]_i, \tag{2.3}$$

where $\mathscr{A}$ is the antisymmetrizer, and ϕ_α, ϕ_t and ϕ_n are wave functions of α, triton, the valence neutron, respectively. Here, $\{\boldsymbol{r}_i\}$ represents spatial coordinates of nucleons, and each nucleon is described as locally shifted Gaussian. $\boldsymbol{R}_i$ is the Gaussian center parameter which is fixed randomly.

The z components of the spins of the two valence neutrons are introduced to be parallel or anti-parallel dependent on the basis state. The index i in Eqs. (2.2) and (2.3) specifies a set of Gaussian center parameters for $\boldsymbol{R}_1$, $\boldsymbol{R}_2$, $\boldsymbol{R}_3$, and $\boldsymbol{R}_4$, and spin directions of valence neutrons. The value of M specifies the z component of the angular momentum in the laboratory frame, and the energy does not depend on M; however, the energy depends on K, which is a z component of the angular momentum in the body-fixed frame.

Next, the differential cross section is obtained by the microscopic coupled-channel (MCC) calculation. The diagonal and transition potentials for the MCC calculation are derived from the microscopic view point. The microscopic potentials have usually the direct ($U^{(D)}$) and exchange ($U^{(EX)}$) parts as

$$U_{\alpha(ij)\to\beta(kl)} = U^{(D)}_{\alpha(ij)\to\beta(kl)} + U^{(EX)}_{\alpha(ij)\to\beta(kl)}, \tag{2.4}$$

where, α and β represent the channel numbers and i, j, k, and l mean the states of the projectile or target nuclei. The direct part of the potential is described by

$$U^{(D)}_{\alpha(ij)\to\beta(kl)}(\boldsymbol{R}) = \int \rho^{(P)}_{i\to k}(\boldsymbol{r_P})\rho^{(T)}_{j\to l}(\boldsymbol{r_T})v_D(\boldsymbol{s},\rho,E)d\boldsymbol{r_P}d\boldsymbol{r_T}, \tag{2.5}$$

and, the exchange part is described by

$$U^{(EX)}_{\alpha(ij)\to\beta(kl)}(\boldsymbol{R}) = \int \rho^{(P)}_{i\to k}(\boldsymbol{r_P},\boldsymbol{r_P}-\boldsymbol{s})\rho^{(T)}_{j\to l}(\boldsymbol{r_T},\boldsymbol{r_T}+\boldsymbol{s})v_{EX}(\boldsymbol{s},\rho,E)\exp(\frac{i\boldsymbol{k}(\boldsymbol{R})\cdot\boldsymbol{s}}{M})d\boldsymbol{r_P}d\boldsymbol{r_T}. \tag{2.6}$$

Here, $\boldsymbol{s} = \boldsymbol{r_P} + \boldsymbol{R} - \boldsymbol{r_T}$. $\boldsymbol{k}(\boldsymbol{R})$ is the local momentum for the nucleus-nucleus relative motion. M is the reduced mass for the reaction system. The subscripts, P and T, for the transition density $\rho^{(P,T)}_{a\to b}$ mean the projectile and target nuclei, respectively. The $v_{D,EX}$ are the direct and exchange part of the effective nucleon-nucleon interaction. In this work, we apply the MPa interaction [8] to the MCC calculation. The ρ and E in the interaction $v_{D,EX}$ are the local density and the incident energy per nucleon.

3. Results

First, we show the calculated excitation energy with the SMCM method in Fig. 1. The left hand side shows the comparison of the experimental data and calculated results for the ^{9}Li nucleus. The right hand side shows the results for the ^{10}Be nucleus. The calculated ^{10}Be results well reproduce the data. On the other hand, the experimental spin assignment is not completed for the ^{9}Li nucleus. However, the calculated result well reproduce the excitation energy. The calculated excitation energies of the ^{10}Be nucleus are 3.247, 5.278, 8.552, 8.692, 10.13, 10.40, 10.74, 10.83 and 13.07 MeV for the 2^+_1, 2^+_2, 3^+_1, 0^+_2, 2^+_3, 4^+_1, 0^+_3, 2^+_4 and 4^+_2 states, respectively. On the other hand, the calculated excitation energies of the ^{9}Li nucleus are obtained as 3.295, 3.337, 4.773 and 5.401 MeV for the $1/2^-_1$, $5/2^-_1$, $7/2^-_1$ and $3/2^-_2$ states, respectively.

Next, we show the nuclear radius for the ground state (g.s.) of the ^{10}Be and ^{9}Li nuclei. The calculated results are compared with the experimental data in Table 1. The calculated ^{9}Li nucleus well reproduce the data but the ^{10}Be nucleus slightly overestimates the experimental data. The neutron part of the ^{10}Be and ^{9}Li nuclei give the comparable result with each other.

Here, we show the transition strengths (B(E2) and B(IS2)) from the excited state to the g.s. in Table 2. The calculated B(E2) value from the 2^+_1 state to the g.s. for the ^{10}Be nucleus well

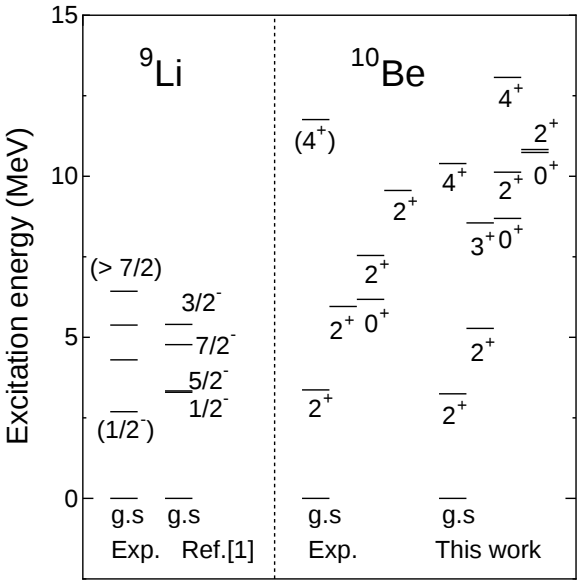

Figure 1: Comparison the calculated excitation energy with the experimental data. The experimental data is taken from Refs. [9].

^{9}Li	proton (fm)	neutron (fm)	matter (fm)
Exp.			
Ref. [10]	2.18(2)	2.39(2)	2.32(2)
Ref. [11]	2.11(4)	2.59(9)	2.44(6)
Calc.			
This work	2.237	2.562	2.459
^{10}Be	proton (fm)	neutron (fm)	matter (fm)
Exp.			
Ref. [10]	2.24(2)	2.34(2)	2.30(2)
Calc.			
This work	2.447	2.631	2.559

Table 1: The calculated nuclear radius compared with the experimental data for the ground state.

reproduce the data. The B(IS2) value from the 2^+_1 state to the g.s. for the ^{10}Be shows the largest value in Table 2. However, the sum of the transition strength for the ^{9}Li nucleus is larger than that for the ^{10}Be nucleus. The B(IS2) value from the 2^+_1 state to the g.s. for the ^{10}Be nucleus and the B(IS2) value from the $1/2^-_1$ state to the g.s. for the ^{9}Li nucleus are comparable. However, it is indicated that the $3/2^-_1$ and $3/2^-_2$ states for the ^{9}Li are agree with the 2^+_1 and 2^+_2 states for the ^{10}Be nucleus from the viewpoint of the microscopic cluster model as discussed in Ref. [4]. Therefore, the agreement of the transition strengths for the ^{9}Li and ^{10}Be nuclei is not important for the nuclear structure sense.

Next, we compare the ^{10}Be nucleus with the ^{9}Li nucleus in the elastic scattering by the ^{12}C target at $E/A = 59.4$ MeV. In the MCC calculation, we take into account the 0^+_1, 2^+_1 and 2^+_2 states for the ^{10}Be nucleus. On the other hand, the $3/2^-_1$, $1/2^-_1$, $5/2^-_1$ and $7/2^-_1$ states are included in

^{9}Li	B(E2) (e^2fm^4)	B(IS2) (fm^4)
Calc.		
$1/2^-_1 \rightarrow$ g.s.	8.778	38.51
$5/2^-_1 \rightarrow$ g.s.	0.5844	12.79
$7/2^-_1 \rightarrow$ g.s.	1.156	15.78
^{10}Be	B(E2) (e^2fm^4)	B(IS2) (fm^4)
Exp.		
Ref. [12]	10.24(97)	
Calc.		
$2^+_1 \rightarrow$ g.s.	11.27	46.84
$2^+_2 \rightarrow$ g.s.	0.7429	0.3551

Table 2: Transition strength from the excited state to the g.s. for the ^{10}Be and ^{9}Li nuclei.

our calculation for the ^{9}Li elastic scattering. The transition density for the ^{12}C nucleus is taken from Ref. [13]. For the ^{12}C nucleus, we take into account the excitation of the 2^+_1 ($E_x = 4.44$ MeV), 0^+_2 ($E_x = 7.65$ MeV), 3^-_1 ($E_x = 9.64$ MeV) states. In this paper, the result including the full combination of projectile and target excitations is called as full-CC calculation.

The renormalization factor is often introduced to reproduce the data by increasing/reducing the real and imaginary parts of the folding model potential. In this work, we apply the renormalization factor only to the imaginary part, as follows;

$$U = V + iN_W W, \tag{3.1}$$

where, the V and W are the real and imaginary part of the folding model potential.

Figure 2 shows the calculated elastic cross section for the ^{9}Li + ^{12}C and ^{10}Be + ^{12}C systems at $E/A = 59.4$ MeV. The filled circles are the experimental data for the ^{10}Be + ^{12}C elastic cross section at $E/A = 59.4$ MeV. The dotted and solid curves are the results by the 1-ch and full-CC calculations, respectively. The dashed curves include the excitation effect of the target nucleus (^{12}C) only. The thin (black) and bold (red) curves are the result of the calculated ^{10}Be and ^{9}Li elastic scatterings, respectively. When we take into account no projectile (^{10}Be and ^{9}Li) excitation effect, the calculated elastic cross sections (dotted and dashed curves) show the similarity of the ^{10}Be and ^{9}Li nuclei. Here, we should note that the horizontal axis is set to be transfer momentum and the vertical axis is set to be absolute value. This setting gives the opportunity to compare the ^{10}Be and ^{9}Li nuclei for the angular distribution.

However, the solid curves including the projectile (^{10}Be and ^{9}Li) excitation effect show the large different channel coupling (CC) effect. Here, the sum of the transition strengths for the ^{9}Li nucleus is clearly larger than that for the ^{10}Be nucleus as shown in Table 2. Therefore, this result by the nuclear reaction calculation is seemingly inconsistent with the information of the nuclear structure.

Here, we show the transition strength from the g.s. to the excited state for the ^{10}Be and ^{9}Li nuclei. The difference between Table 2 and Table 3 is the transition direction only. Table 3 shows the large transition strength of the ^{10}Be nucleus. This transition strength is consistent with the MCC

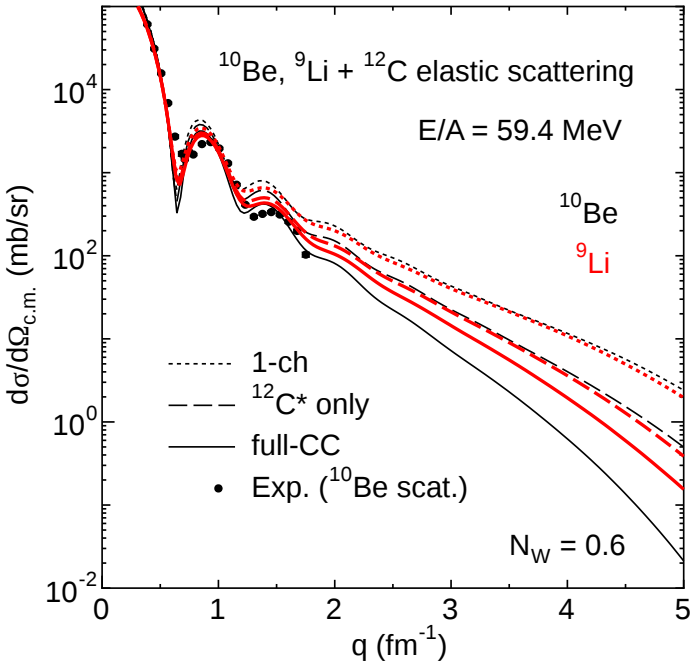

Figure 2: Elastic cross section for the ^{9}Li + ^{12}C and ^{10}Be + ^{12}C systems at $E/A = 59.4$ MeV. The experimental data is taken from Ref. [14]

^{9}Li	B(E2) (e^2fm^4)	B(IS2) (fm^4)
Calc.		
g.s. $\to 1/2^-_1$	4.389	19.26
g.s. $\to 5/2^-_1$	0.8766	19.19
g.s. $\to 7/2^-_1$	2.313	31.55
^{10}Be	B(E2) (e^2fm^4)	B(IS2) (fm^4)
Calc.		
g.s. $\to 2^+_1$	56.35	234.2
g.s. $\to 2^+_2$	3.714	1.776

Table 3: Transition strength from the g.s. to the excited state for the ^{10}Be and ^{9}Li nuclei.

result shown in Fig. 2. The initial states of the projectile and target are ground state in the nuclear reaction. After the collision, the projectile and target nuclei can be excited. In such situation, the important transition direction is from the g.s. to the excited state from the viewpoint of the nuclear reaction. Finally, the transition strength from the g.s. to the excited state is consistent with the CC effect on the elastic cross section. We here note that the situation are overlooked in Ref. [15] and the study of Ref. [15] could be misleading.

4. Summary

We construct the ^{10}Be and ^{9}Li nuclei with the stochastic multi-configuration mixing (SMCM) method as the $\alpha+\alpha+n+n$ and $\alpha+t+n+n$ four body cluster model, respectively. The calculated

excitation energy, nuclear radius and transition strength well reproduce the experimental data. With the wave functions, the ^{10}Be and ^{9}Li elastic cross sections by the ^{12}C target nucleus are obtained with the microscopic coupled channel (MCC) calculation. The ^{10}Be and ^{9}Li elastic cross sections are closed to each other without the CC effect. However, their angular distributions show the different CC effect when their excitation effects are taken into account in the MCC calculation. The CC effect for ^{10}Be scattering is larger than that for the ^{9}Li nucleus nevertheless the sum of the transition strengths from the excited state to ground state (g.s.) for the ^{9}Li nucleus is clearly larger than that for the ^{10}Be nucleus. Then, We found the reason why the transition strength are inconsistent with the CC effect on the elastic cross section. The transition strength from the excited state to the g.s. are firstly shown. The transition strength is dependent on the transition direction and the important transition direction is found to be from the g.s. to the excited state in the CC effect on the elastic cross section. In addition, the spin of the ground and excited states is completely different in the comparison of the ^{10}Be and ^{9}Li nuclei. Finally, we obtain the consistent result of the nuclear structure and reaction models with the caution.

5. Acknowledgements

This work was supported by JSPS KAKENHI Grant Numbers JP15H00842, JP15K17661, JP15K17662, and JP26400269.

References

[1] N. Itagaki and S. Okabe, *Phys. Rev. C* **61**, 044306, 2000.

[2] K. Arai, Y. Ogawa, Y. Suzuki and K. Varga, *Prog. Theor. Phys. Suppl.* **142**, 97, 2001.

[3] W. von Oertzen, M. Freer and Y. Kanada-En'yo, *Phys. Rep.* **432**, 43, 2006.

[4] T. Furumoto, T. Suhara and N. Itagaki, *Phys. Rev. C* **87**, 064320, 2013.

[5] T. Suhara and Y. Kanada-En'yo, *Prog. Theor. Phys.* **123**, 303, 2010.

[6] Y. Kanada-En'yo and T. Suhara, *Phys. Rev. C* **85**, 024303, 2012.

[7] Y. Kanada-En'yo, *Phys. Rev. C* **94**, 024326, 2016.

[8] Y. Yamamoto, T. Furumoto, N. Yasutake and Th.A. Rijken, *Phys. Rev. C* **90**, 045805, 2014.

[9] National Nuclear Data Center, *http://www.nndc.bnl.gov/.*

[10] I. Tanihata et. al., *Phys. Lett.* **B206**, 592, 1988.

[11] A. V. Dobrovolsky et. al., *Nucl. Phys.* **A766**, 1, 2006.

[12] F. Ajzenberg-Selvo and J.H. Kelley, *Nucl. Phys.* **A506**, 1, 1990.

[13] M. Kamimura, *Nucl. Phys.* **A351**, 456, 1981.

[14] Experimental Nuclear Reaction Data (EXFOR), *http://www.jcprg.org/exfor/.*

[15] T. Furumoto, T. Suhara and N. Itagaki, *Proceedings of 11th International Conference on Clustering Aspects of Nuclear Reactions and Dynamics*, in press.